A novel *ANO5* splicing variant in a LGMD2L patient leads to production of a truncated aggregation-prone Ano5 peptide

Jing Xu[1][†], Li Xu[1][†], Yeh S Lau[1], Yandi Gao[1], Steven A Moore[2] and Renzhi Han[1]* 🔘

[1] *Division of Cardiovascular Medicine, Department of Cardiac Surgery, Dorothy M. Davis Heart and Lung Research Institute, The Ohio State University Wexner Medical Center, Columbus, OH, USA*
[2] *Department of Pathology, Carver College of Medicine, University of Iowa, Iowa City, IA, USA*

Correspondence to: Renzhi Han, Department of Cardiac Surgery, Davis Heart and Lung Research Institute, The Ohio State University Wexner Medical Center, Biomedical Research Tower 316, Columbus, OH 43210, USA. E-mail: renzhi.han@osumc.edu

[†] *These authors contributed equally to this work.*

Abstract

Mutations in *ANO5* cause several human diseases including gnathodiaphyseal dysplasia 1 (GDD1), limb-girdle muscular dystrophy 2L (LGMD2L), and Miyoshi myopathy 3 (MMD3). Previous work showed that complete genetic disruption of *Ano5* in mice did not recapitulate human muscular dystrophy, while residual expression of mutant *Ano5* in a gene trapped mouse developed muscular dystrophy with defective membrane repair. This suggests that truncated Ano5 expression may be pathogenic. Here, we screened a panel of commercial anti-Ano5 antibodies using a recombinant adenovirus expressing human Ano5 with FLAG and YFP at the N- and C-terminus, respectively. The monoclonal antibody (mAb) N421A/85 was found to specifically detect human Ano5 by immunoblotting and immunofluorescence staining. The antigen epitope was mapped to a region of 28 residues within the N-terminus. Immunofluorescence staining of muscle cryosections from healthy control subjects showed that Ano5 is localized at the sarcoplasmic reticulum. The muscle biopsy from a LGMD2L patient homozygous for the c.191dupA mutation showed no Ano5 signal, confirming the specificity of the N421A/85 antibody. Surprisingly, strong Ano5 signal was detected in a patient with compound heterozygous mutations (c.191dupA and a novel splice donor site variant c.363 + 4A > G at the exon 6–intron 6 junction). Interestingly, insertion of the mutant intron 6, but not the wild-type intron 6, into human *ANO5* cDNA resulted in a major transcript that carried the first 158-bp of intron 6. Transfection of the construct encoding the first 121 amino acids into C2C12 cells resulted in protein aggregate formation, suggesting that aggregate-forming Ano5 peptide may contribute to the pathogenesis of muscular dystrophy.

Keywords: aggregate; anoctamin; Ano5; LGMD2L; muscular dystrophy; TMEM16

Introduction

Anoctamin 5 (Ano5), also known as transmembrane protein 16E (TMEM16E) and gnathodiaphyseal dysplasia 1 (GDD1), belongs to the anoctamin protein family. *ANO5* was initially identified as the causative gene for the late-onset GDD [1], in which the cysteine residue at amino acid position 356 is mutated to glycine or arginine. Subsequently, the physiological importance of this gene in muscle was shown by the presence of recessive *ANO5* mutations in individuals with anoctaminopathy: limb-girdle muscular dystrophy (LGMD2L) and Miyoshi myopathy (MMD3) [2,3]. A recent cohort analysis of 786, mostly Italian,

patients with a clinical diagnosis of LGMD or other, genetically undefined, myopathies found that 4% had two mutant *ANO5* alleles; another 3% of the patients were heterozygous [4]. A prevalence of 2/100,000 has been estimated for anoctaminopathy in Finland [2]. Interestingly, complete genetic disruption of *Ano5* in mice did not recapitulate human muscular dystrophy [5,6], while residual expression of mutant *Ano5* in a gene-trapped mouse was found to result in the development of muscular dystrophy with defective membrane repair [7].

The anoctamin protein family includes a total of 10 proteins (Ano1 to 10, or TMEM16A to H, J, and K) [8,9]. A topological analysis of Ano5 based on its amino acid sequence suggested that it carries eight

transmembrane regions. However, a recent structural analysis [10] revealed that an Ano6 ortholog from the fungus *Nectria haematococca* carries 10 transmembrane regions. The members of the anoctamin family were shown to be Ca^{2+}-activated proteins with putative functions as either ion channels or lipid scramblases or both [11,12]. Although the functional analysis of Ano5 failed to find it has plasma membrane Ca^{2+}-activated chloride channel activity [13,14], which was originally identified in Ano1 and Ano2 [13,15–17], sequence comparison indicated that Ano5 carries a segment composed of 35 amino acids homologous to the scrambling domain in Ano6 [6,18]. When this 35-amino-acid segment of Ano5 replaced the corresponding segment of Ano1, the chimeric molecule showed Ca^{2+}-dependent scrambling. This evidence suggested that Ano5 might function as a phospholipid scramblase.

In human and murine tissues, the *ANO5* gene shows abundant expression in skeletal muscle, bone, and testis [1,19–22]. Previous studies with the epitope-tagged Ano5 protein in cultured cells revealed an endoplasmic reticulum (ER) localization [21,23]. Moreover, Ano5 was rapidly degraded by the proteasome pathway [14]. Our previous study showed that Ano5 is not required for myoblast proliferation or differentiation [24]. Due to the lack of reliable antibodies and conflicting phenotypes in the knockout mouse models, it remains a challenge to determine the biochemical functions of Ano5 protein and elucidate the molecular pathophysiology of Ano5-related muscular dystrophy.

As an important step toward elucidating the pathogenesis of the anoctaminopathies and understanding the molecular functions of Ano5, we conducted a series of experiments aimed at identifying reliable anti-Ano5 antibodies that could specifically detect human Ano5 protein expressed exogenously. We further characterized the expression and localization of endogenous Ano5 from human patients using a validated monoclonal antibody (mAb), and identified a splicing mutation leading to the production of a truncated Ano5 peptide which is prone to form aggregates that may be pathogenic.

Materials and methods

Plasmid construction

Overlapping extension polymerase chain reaction (PCR) was used to amplify truncated *ANO5* fragments. In each reaction, 50 μl PCRs contained 1 ng human *ANO5* cDNA as template, 5 μl 10× AccuPrime™ PCR Buffer I, 1 μl AccuPrime™ Taq DNA Polymerase (Invitrogen, Carlsbad, CA, USA) and 1 μM primers. Reaction conditions were 35 cycles of 15 s at 95 °C, 30 s at 60 °C, and 1 min at 68 °C, followed by 5 min at 68 °C. The PCR fragments were subcloned into pEGFP-N1 vector. To construct full-length human *ANO5* with either wild-type or mutant intron 6, the intron 6 was amplified by overlapping extension PCR. The fusion PCR products were subcloned into the pLKO-3Flag-hANO5-EGFP vector. All plasmids were verified by both restriction enzymatic digestion and Sanger sequencing. The primers used in the study are listed in supplementary material, Table S1.

Cell culture and transfection

HEK293 cells were cultured in Dulbecco's modified eagle's medium (DMEM) (Sigma, St. Louis, MO, USA) containing 10% fetal bovine serum (FBS) and 1% penicillin–streptomycin (Invitrogen). Cells were plated in 6-well plates and transfected with the designated plasmids by polyethylenimine (PEI) as previously described. After 48 h, cells were analysed by western blotting and reverse transcriptase PCR (RT-PCR).

RNA and quantitative RT-PCR analysis

Total RNA was extracted from HEK293 cells and treated with DNase I by using Zymo Quick-RNA™ MiniPrep kit (Zymo Research Corporation, Irvine, CA, USA) following the manufacturer's protocol. Total RNA was used as template for first-strand cDNA synthesis by using RevertAid RT Reverse Transcription Kit (Life Technologies, Carlsbad, CA, USA). RT-PCR was performed using AccuPrime™ Taq DNA Polymerase (Invitrogen) and the RT-PCR product from the *ANO5* construct with the mutant intron 6 was sequenced at Genomics Shared Resource, The Ohio State University.

Adenovirus generation and transduction

FLAG-hANO5-YFP or EGFP were subcloned into pShuttle-CMV vectors (Clontech, Mountain View, CA, USA) and recombinant adenovirus genomic DNA was generated using the AdEasy-1 Adenovirus system (Agilent Technologies, La Jolla, CA, USA) according to the manufacturer's instructions as previously described. The adenoviral particles were packaged and amplified in AD293 cells. At 72 h postinfection, the amplified virus was harvested by freeze-thawing three times and centrifuged at 4 °C for 15 min. The concentrated viruses were used to infect AD293 cells at 70% confluence.

Lentiviral generation and transduction

Mouse Ano5-mCherry or mCherry-C1 cassettes were subcloned into pLVX-mCherry-C1 vector (Clontech) for making Ano5 lentiviruses. The lentiviral vectors were co-transfected with ViraPower lentiviral packaging mix plasmids (Invitrogen) into virus-producing 293T cells. After 48 h, the supernatants were harvested. AD293 were transduced with the recombinant lentiviral particles in the presence of 8 mg/ml polybrene (Sigma). Two days after lentivirus transduction, the cells were selected for about a week with 1 μg/ml puromycin in the culture media.

Immunocytochemistry and confocal imaging

HEK293 cells were plated in 4-well glass slide chambers (Iwaki Glass, Tokyo, Japan) and infected with Ad-GFP or Ad-FLAG-hANO5-YFP at 70% confluence. At 24 h after infection, cells were washed twice with cold phosphate-buffered saline (PBS) and fixed in 4% paraformaldehyde (Nacalai Tesque, San Diego, CA, USA)) at room temperature for 15 min. Skeletal muscle cryosections of human patients were similarly prepared. Fixed cells and cryosections were then washed with PBS and incubated with blocking solution (PBS, 2% BSA, 0.5% Triton X-100, 0.1% Tween 20) for 1 h before overnight incubation at 4 °C with mouse monoclonal anti-Ano5 antibody (N421A/85, 1:100; UC Davis/NIH NeuroMab Facility, Davis, CA, USA), rabbit polyclonal anti-Calnexin antibody (ab22595, 1:400; Abcam, Cambridge, MA, USA), or rabbit polyclonal anti-dystrophin antibody (Ab15277, 1:400; Abcam). Cells and slides were then extensively washed with PBS and incubated with secondary antibodies (AlexaFluor 555 goat anti-mouse IgG, A-21422, Invitrogen, 1:400; AlexaFluor 594 goat anti-rabbit IgG, A-11037, Invitrogen, 1:400) for 1 h at room temperature. Finally, the cells were mounted using VECTASHIELD® Mounting Medium with 4′,6-diamidino-2-phenylindole (DAPI) (Vector Laboratories, Inc., Burlingame, CA, USA). Images were taken and analysed using a Zeiss 780 confocal microscope (Carl Zeiss AG, Oberkochen, Germany).

Western blotting

Cells and frozen tissue sections were lysed in cold RIPA buffer [20 mM Tris-HCl (pH 7.5), 150 mM NaCl, 1 mM EDTA, 1 mM EGTA, 1% NP-40, 1% sodium deoxycholate, 2.5 mM sodium pyrophosphate, 1 mM b-glycerophosphate, 1 mM Na_3VO_4, 1 μg/ml leupeptin] supplemented with protease inhibitors [protease inhibitor mixture (Sigma) and 1 mM phenylmethylsulfonyl fluoride]. Extracted protein samples were separated by SDS-PAGE (4–20%) and transferred onto polyvinylidene fluoride (PVDF) membranes (0.45 μm). Membranes were blocked with 5% (v/v) nonfat dry milk in Tris-buffered saline with Tween 20 [TBST; 20 mM Tris-HCl (pH 7.6), 150 mM NaCl, 0.1% Tween 20] at room temperature for 1 h and incubated with primary antibodies (detailed information for the primary antibodies used in this study is provided in supplementary material, Table S2) at 4 °C overnight. Then, membranes were washed with TBST and incubated with secondary antibodies at room temperature for 1.5 h. After washing with TBST, the membranes were developed using ECL western blotting substrate (Pierce Biotechnology, Rockford, IL, USA) and exposed to Chemi-Doc™ XRS+ Imaging System (Bio-Rad Laboratories, CA, USA) and analysed with ImageLab™ Software (Bio-Rad Laboratories).

Results

Western blot validation of anti–Ano5 antibodies using exogenously expressed Ano5 fusion proteins

Previous studies showed that Ano5 was rapidly degraded via the proteasome pathway and transient transfection with a plasmid encoding Ano5-GFP resulted in very low GFP fluorescence [14], despite the high transfection efficiency. To validate the antibodies raised against human/mouse Ano5 antigens, we constructed a recombinant adenovirus (Ad) expressing human Ano5 with FLAG and YFP tags at the N- and C-terminus, respectively. At 24 h after the infection of AD293 cells with Ad-FLAG-hANO5-YFP, most cells showed clear YFP fluorescence (supplementary material, Figure S1A). The anti-FLAG and anti-GFP antibodies detected a major band migrating at ~130 kDa in the cell lysate with Ad-FLAG-hANO5-YFP transduction (Figure 1A,B). This band size is consistent with the predicted molecular mass of the FLAG-hANO5-YFP fusion protein. In addition, both antibodies detected a higher band at ~280 kDa, which is likely the dimeric form or aggregate of the fusion protein. Interestingly, the anti-GFP antibody also detected an additional band at ~60 kDa, while the anti-FLAG antibody recognized several other smaller bands at ~50, 37, and 22 kDa. Since the YFP (~28 kDa) is located in the C-terminus while the FLAG tag (~1.3 kDa) is located in the N-terminus, these results indicate that the Ano5 protein is likely cleaved into a ~32 kDa C-terminal fragment and several N-terminal fragments with molecular masses at ~49, 36, and 21 kDa.
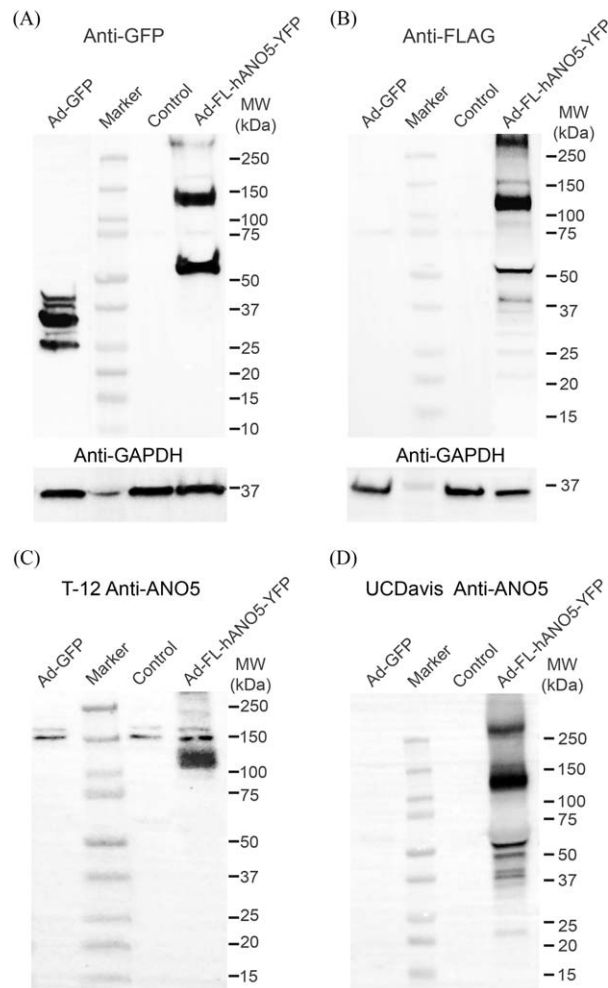
Figure 1. Screening of the anti–Ano5 antibodies by western blotting analysis. AD293 cells infected with adenoviruses expressing GFP or FLAG-hANO5-YFP were analysed by western blotting with anti-GFP (A), anti-FLAG (B), Santa Cruz T-12 anti-Ano5 (C), UC Davis/NIH NeuroMab Facility anti-Ano5 (D), or GAPDH (bottom panel in A and B). The molecular mass standards (Precision Plus Standard; Bio-Rad) are shown in kilodalton on the right for each panel. All experiments were repeated at least three times.

We then screened five commercial anti-Ano5 antibodies (supplementary material, Table S1) by western blot. The anti-Ano5 antibodies from Santa Cruz Biotechnology (Dallas, Texas, USA) (K-13), Abcam (ab188116), and Abgent (AP8580B) all failed to yield any specific band for the human *ANO5* fusion construct (supplementary material, Figure S2). The polyclonal T-12 antibody from Santa Cruz Biotechnology weakly recognized the human Ano5 fusion protein (Figure 1C). The mAb N421A/85 from the UC Davis/NIH NeuroMab Facility can strongly and specifically detect the human Ano5 fusion protein expressed in AD293 cells with a lower exposure as

compared to T-12 antibody (Figure 1D). In addition to the predicted full-length band at ∼130 kDa, the N421A/85 antibody also detected a larger band at ∼280 kDa and several smaller bands ranging from 22 to 50 kDa (Figure 1D), similar to those observed with the anti-FLAG antibody. This is consistent with the antigen for N421A/85 being located at the N-terminus of human Ano5.

To test if these antibodies also recognize mouse Ano5, we generated a stable cell line expressing mouse Ano5 fused with mCherry at the N-terminus (supplementary material, Figure S1B). The T-12 antibody did not recognize the mCherry-mAno5 fusion protein although both the dsRed and N421A/85 antibodies showed a specific band at ∼130 kDa, matching the size of the full-length fusion protein (supplementary material, Figure S3). Two smaller bands of ∼75 and 50 kDa were also clearly observed, which correspond to the bands of ∼50 and 22 kDa from FLAG-hANO5-YFP adenovirus infected AD293 cells after subtracting the molecular mass of the tags. Overall, the western blotting results indicate that the monoclonal N421A/85 antibody can specifically recognize exogenously expressed human and mouse Ano5 with high sensitivity, and that both human and mouse Ano5 are proteolytically cleaved into smaller N- and C-terminal fragments.

Examination of exogenously expressed Ano5 by immunofluorescence staining with the N421A/85 mAb

To examine whether the N421A/85 antibody can be used to detect human Ano5 by immunofluorescence staining, we infected AD293 cells with Ad-GFP or Ad-FLAG-hANO5-YFP, and stained the cells with the N421A/85 antibody. Fluorescence microscopy showed that the N421A/85 antibody can specifically detect exogenously expressed human Ano5 by immunofluorescence staining (Figure 2A). We further investigated whether Ano5 is localized at the ER by co-labelling the cells with the N421A/85 antibody and an ER-specific marker calnexin [25]. The FLAG-hANO5-YFP protein was mostly found at intracellular membranes and partially co-localized with calnexin (Figure 2A,B), suggesting that Ano5 resides on the ER membrane.

Mapping the epitope of the N421A/85 antibody

The monoclonal N421A/85 antibody was raised against the entire N-terminal fragment of human Ano5 (∼300 amino acids). To further map the epitope for this antibody, we generated eight truncated
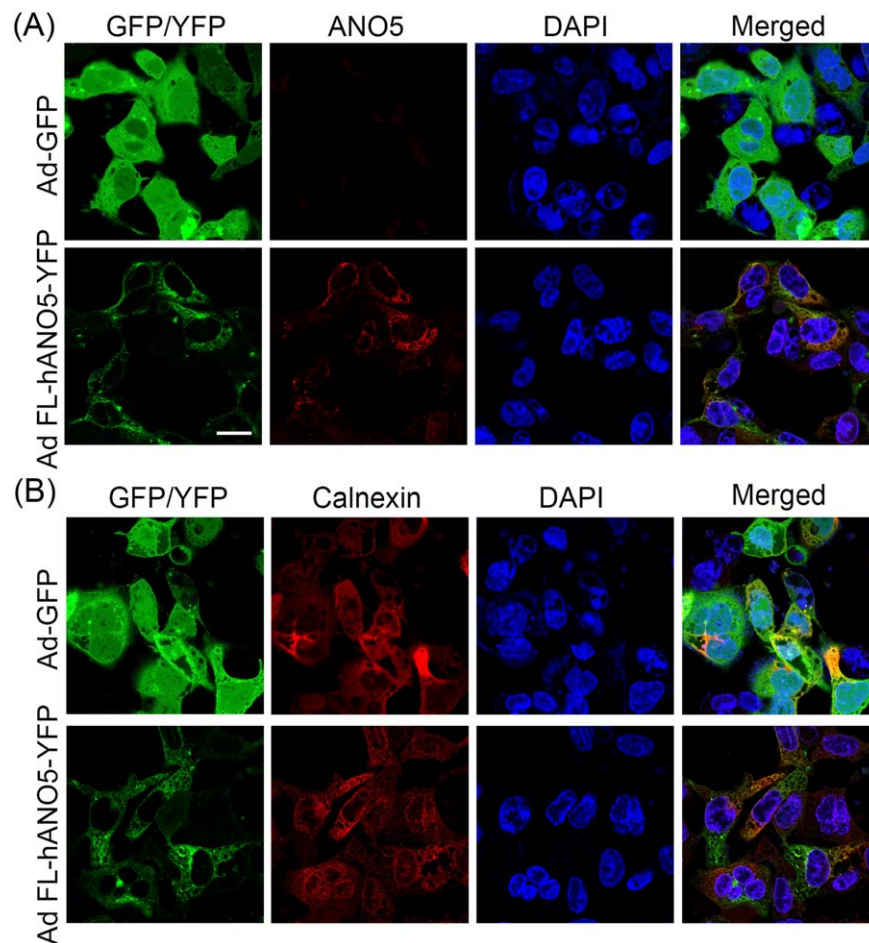
Figure 2. Confocal imaging of recombinant Ano5 immunostained using N421A/85 Ab. (A) AD293 cells infected with adenoviruses expressing GFP or FLAG-hANO5-YFP were stained with anti-Ano5 antibody (N421A/85, red) and DAPI (blue). The green signals represent the expression of GFP or FLAG-hANO5-YFP. (B) AD293 cells infected with adenoviruses expressing GFP or FLAG-hANO5-YFP were stained with anti-calnexin (an ER marker) antibody (red) and DAPI (blue). GFP or FLAG-hANO5-YFP is shown in green. Scale bar = 10 μm. These are representative of a minimum of three experiments.

N-terminal fragments of human Ano5, each tagged with FLAG and GFP at the N- and C-terminus, respectively (Figure 3A). AD293 cells were transfected with GFP control or individual truncated Ano5 constructs. When examined for GFP fluorescence with fluorescence microscopy, the expression level varied significantly for the truncated Ano5 fragments (supplementary material, Figure S4). In particular, the expression level decreased with the length of the constructs, and the one containing the first 64 amino acids exhibited the highest GFP signal. Construct #2 (1–121 amino acids) was highly prone to form cytoplasmic aggregates. These results suggested that the cytoplasmic N-terminal tail of Ano5 is important for its expression and stability. As shown in Figure 3, both the anti-GFP and anti-FLAG antibodies can recognize all the constructs of Ano5. We observed that the constructs carrying the first 121 amino acids or

beyond but not the one carrying the first 64 amino acids of human Ano5 were recognized by the N421A/85 antibody. Moreover, the N421A/85 antibody strongly detected construct #8 which carries only 28 amino acids from position 79 to 106 (QIDFVLSYVDDVKKDAELKAERRKEFET). Further truncation of the last eight amino acids, which are encoded by exon 6, yielded no signal (data not shown). These results indicate that the immunogen for the N421A/85 antibody is located within the region spanning amino acids 79–106 of human Ano5.

Characterization of Ano5 expression in muscle biopsies of human patients

Genetic analysis revealed that most of the muscular dystrophy mutations in *ANO5* are homozygous or compound heterozygous missense mutations, frameshifting
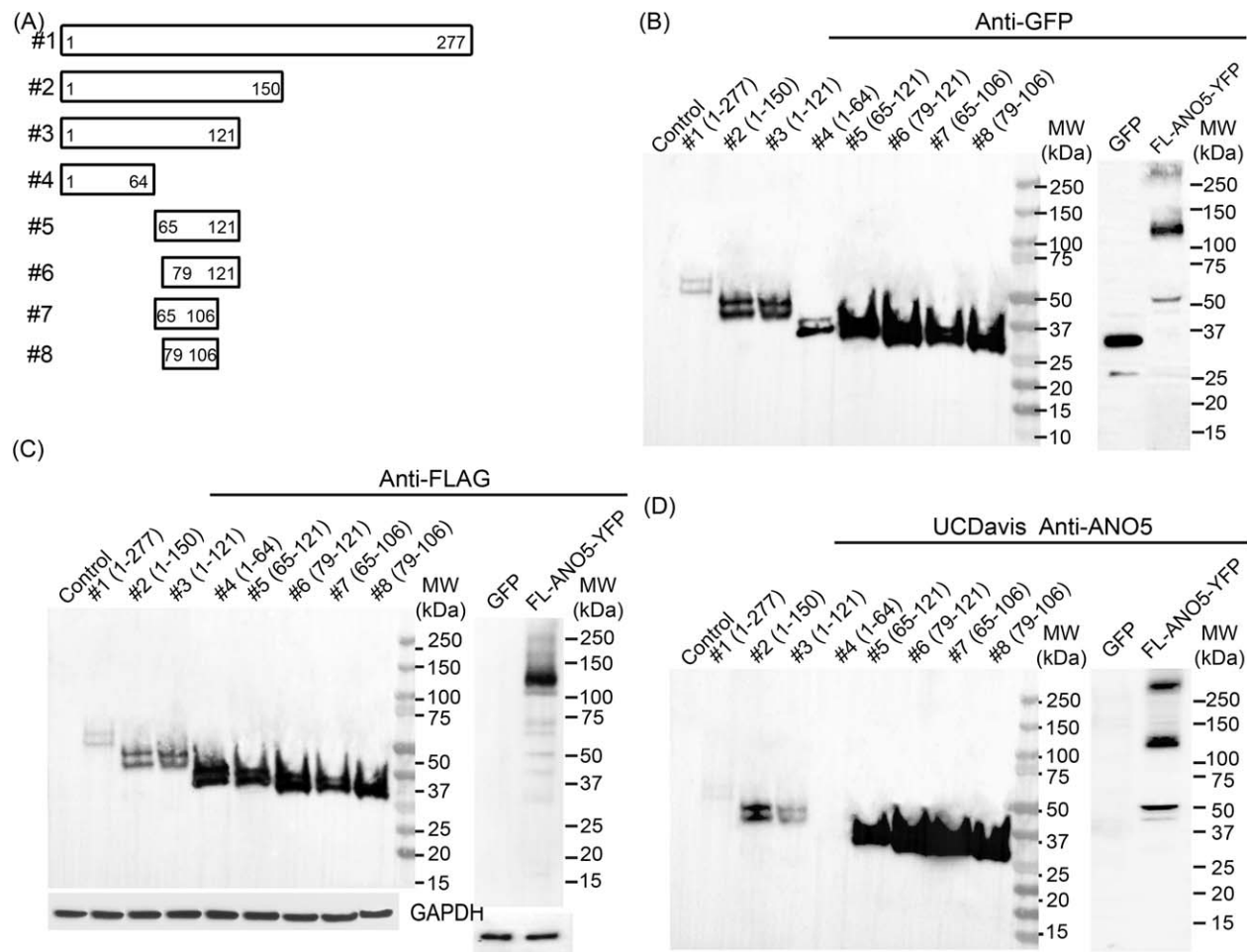
Figure 3. Epitope mapping of the UC Davis anti-Ano5 mAb (N421A/85). (A) Schematic showing different truncated constructs of human Ano5. The numbers in the boxes represent the positions of the amino acids of Ano5. Truncated and full-length constructs expressing recombinant human Ano5 tagged with FLAG and GFP were analysed by western blotting with anti-GFP (B), anti-FLAG (C), or UC Davis anti-Ano5 (N421A/85)(D) antibodies. The loading control of GAPDH for each panel is the same as in panel C. The molecular mass standards (Precision Plus Standard; Bio-Rad) are shown in kilodalton on the right for each panel.

duplication or deletion, or splice site mutations. There are limited data about how these changes affect the protein expression of Ano5 in human patients. Therefore, it was interesting to assess if the N421A/85 antibody is able to detect endogenous Ano5 protein expression by western blot and/or immunofluorescence staining in control and *ANO5*-mutant patients.

We collected muscle biopsies from three unaffected patients (C1–C3) and three LGMD2L patients with confirmed mutations in *ANO5* (P1–P3) (Table 1). Two heterozygous mutations were found in P1: the known mutation c.191dupA in exon 5 causing a frameshift (p.Asn64Lys_fs*15) [2,3,26] and a novel mutation (c.363 + 4A > G) in the splicing donor site of intron 6. All three patients with *ANO5* mutations showed typical muscular dystrophy features including increased fiber size variation (atrophy and hypertrophy), muscle fiber

necrosis and regeneration, endomysial fibrosis, and increased internally placed nuclei (Figure 4A); some muscle fibers contained rimmed vacuoles. The homozygous c.191dupA mutation was found in P2. Since the

Table 1. Clinical and genetic data of the control (C1–3) and ANO5 (P1–3) patients

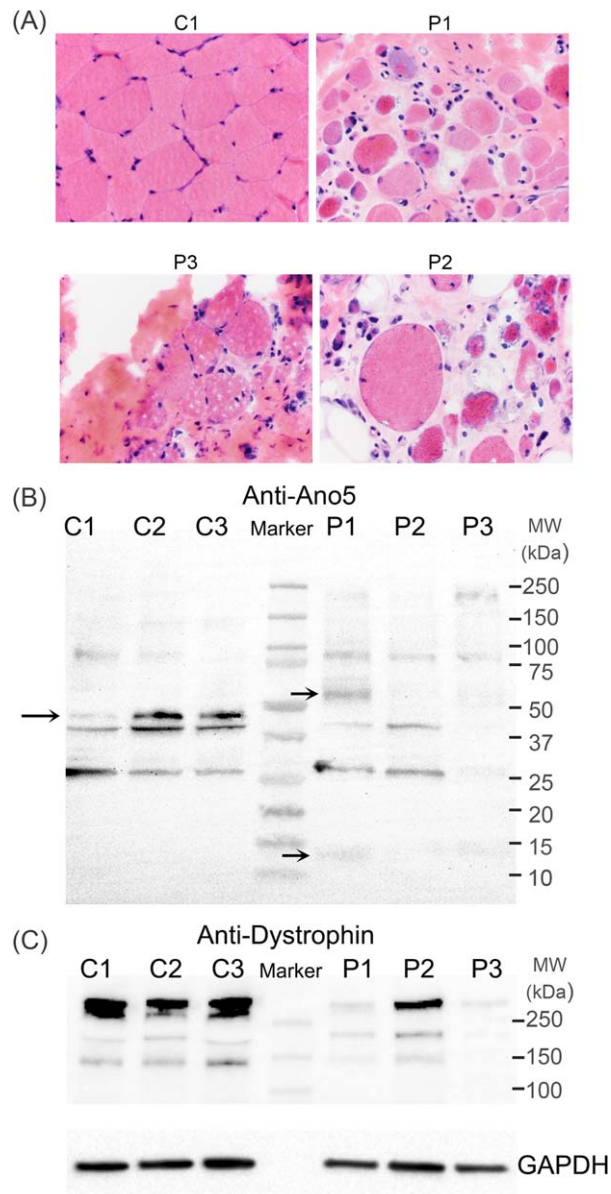| ID	Age (years)	Sex	Allele 1	Allele 2
C1	57	F	NA	NA
C2	40	F	NA	NA
C3	29	F	NA	NA
P1	23	M	c.191dupA; p.N64K_fs*15	c.363 + 4A>G
P2	35	M	c.191dupA; p.N64K_fs*15	c.191dupA; p.N64K_fs*15
P3	32	M	c.172C>T; p.R58W	c.172C>T; p.R58W

NA, not applicable.

Figure 4. Expression of Ano5 in the skeletal muscle biopsies of human patients. (A) H&E staining of human skeletal muscle sections from one control (C1) and three *ANO5* patients (P1–P3). (B) The human skeletal muscle lysates were analysed by SDS-PAGE and immunoblotted with antibodies against Ano5 (B, N421A/85) or dystrophin (C). GAPDH was used as the loading control.

N421/85 mAb did not detect the first 64 residues of human Ano5, we expected that this mAb would not yield any specific signal for P2. This would offer us a negative reference to assure any specific Ano5 signal in the patient samples using this mAb.

To examine the expression of Ano5 in the skeletal muscle of human patients, we performed western blotting analysis of the aforementioned patient samples with the

N421A/85 antibody. The muscle biopsies from the control patients all showed a specific band around 49 kDa, which was not present in both Ano5-patient samples. This 49 kDa band is likely to correspond to the 50 kDa band seen with the recombinant FLAG-hANO5-YFP adenovirus or the 75 kDa band with mCherry-mAno5 (Figure 1 and supplementary material, Figure S2). Interestingly, patient P1 showed two specific bands at ~15 and 60 kDa, which may be due to the aberrant splicing associated with the c.363 + 4A > G mutation. Of note, the predicted full-length Ano5 (107 kDa) was not clearly detected in any muscle samples (Figure 4B), which is different from a recent report [27] and might be due to different methods used to extract proteins. To examine whether this might also be due to non-specific protein degradation, we blotted the samples for dystrophin expression; the C-terminus portion of this 427 kDa muscle protein is known to be prone to degradation. The data show that full-length dystrophin is well detected in all control patient samples, but greatly reduced in two of the Ano5 patient samples (Figure 4C). These data suggest that the full-length Ano5 protein may be very labile as shown previously with the recombinant Ano5 protein [14].

Consistent with previous studies [14,18], our data also show that recombinant Ano5 resides primarily on the ER membrane and intracellular vesicles (Figure 2). To study the expression and subcellular localization of endogenous Ano5 in human muscles, we performed immunofluorescence staining with the N421A/85 antibody and the antibody against dystrophin or calnexin. In contrast to the sarcolemmal staining of dystrophin, Ano5 is restricted to the intracellular membranes (Figure 5), and partially co-localized with the ER marker calnexin in all control patient muscle biopsies (supplementary material, Figure S5).

In line with the western blotting and genotyping results, patient P2 did not show any appreciable Ano5 signal on immunofluorescence staining (Figure 5). Strikingly, patient P1 displayed strong Ano5 signals in the majority of muscle fibers and they formed intracellular aggregates in many muscle fibers (Figure 5). These data suggest that the aberrant splicing of the c.363 + 4A > G mutation leads to strong expression of mutant Ano5 peptide(s), which may be involved in the pathogenesis of muscular degeneration.

Aberrant splicing and production of truncated Ano5 peptide due to c.363 + 4A > G mutation

To gain insight into the mechanism by which the c.363 + 4A > G mutation leads to the production of Ano5 peptides, we performed *in silico* sequence analysis to examine the impact of this mutation on splicing. Using two different splice site predictors [28,29],
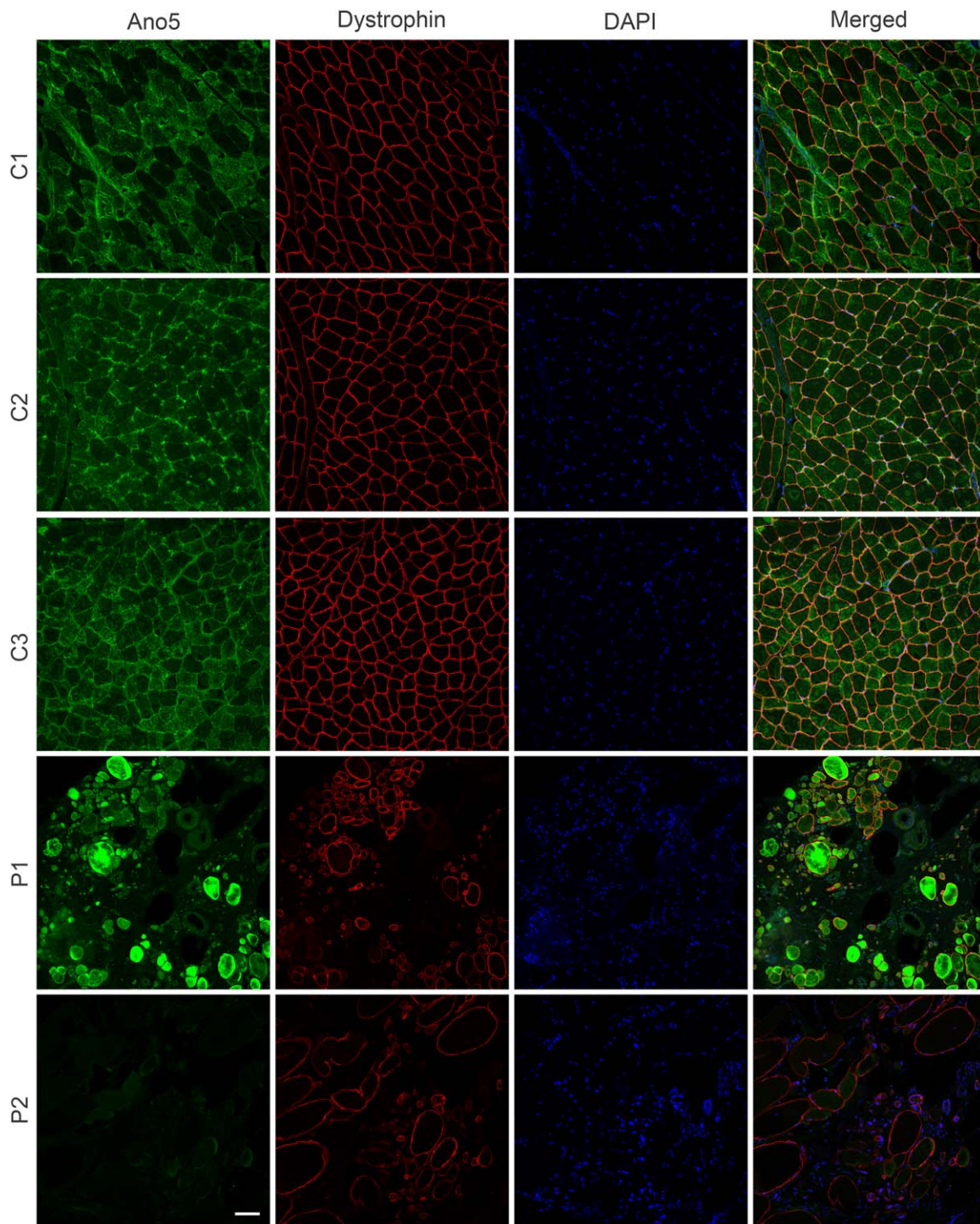
Figure 5. Immunofluorescence analysis of Ano5 in skeletal muscle cryosections from control (C1–3) and *ANO5* (P1, P2) human patients. The human skeletal muscle cryosections were double-stained with antibodies against Ano5 (green, N421A/85) and dystrophin (red). Nuclei were counterstained with DAPI (blue). Scale bar = 100 μm.

we found that the c.363 + 4A > G mutation greatly reduced the likelihood of this splice donor (from 0.97 to 0.75 [28] or from 0.42 to 0 [29]), and a down-stream splicing donor site is predicted to be used in the presence of this mutation, which would splice in a 158-bp sequence from intron 6. Such aberrant splicing
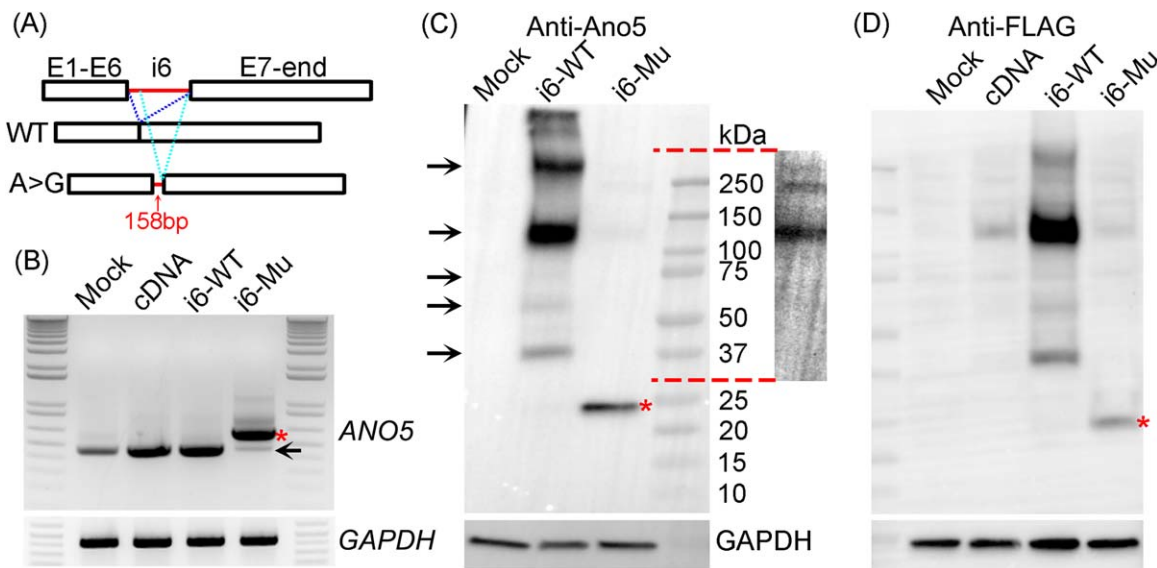
Figure 6. Aberrant splicing and production of truncated Ano5 peptide caused by c.363 + 4A > G mutation. (A) Diagram showing the *ANO5* constructs carrying intron 6 (i6, WT, or mutant) between exons 6 and 7. The WT intron results in correct splicing while the mutant intron is expected to disrupt the splicing site and use a downstream site so that a 158-bp sequence from intron 6 will be included in the cDNA. Red asterisk: mutant transcript; arrow: WT transcript. (B) RT-PCR analysis of *Ano5* expression in cells transfected with different constructs. (C, D) Immunoblotting of cells transfected with the *Ano5* constructs using mAb-Ano5 (C), anti-FLAG (D), and anti-GAPDH. Higher exposure of the upper region of the mutant lane in panel C is shown to the right of the panel. Red asterisk: mutant Ano5 peptide.

would cause pre-mature stop of translation after 11 extra amino acids encoded by this sequence. To test this, we engineered two Ano5 constructs (with an N-terminal FLAG tag and C-terminal GFP) by inserting the 1249-bp WT or c.363 + 4A > G mutant intron 6 into the *ANO5* cDNA sequence between exons 6 and 7 (Figure 6A). By RT-PCR analysis, we found that the construct carrying WT intron 6 showed the same size PCR product as the cDNA without intron 6, indicating that WT intron 6 is correctly spliced out. However, the construct containing mutant intron 6 produced a larger band with several faint bands of different sizes (Figure 6B). Sanger sequencing of the major PCR product showed exactly that the 158-bp sequence was spliced in between exons 6 and 7 (supplementary material, Figure S6). The immunoblotting data showed that the mutant intron 6 resulted in the production of a truncated ~24 kDa peptide (Figure 6C,D).

Discussion

Recessive mutations in *ANO5* have been linked to LGMD2L and MMD3 [26,30,31]. Most of these mutations are homozygous or compound heterozygous, leading to changes of critical amino acids or frameshift/truncation of Ano5. The mutations spread across the *ANO5* gene, with no obvious hot spots in muscular dystrophy patients. Despite clear genetic linkages of *ANO5* to muscular dystrophy, recent studies with genetic mouse models of *Ano5* deficiency showed that they presented little to no muscular dystrophy phenotype. It remains unclear what exactly causes such discrepancy between human and mouse. However, the lack of reliable antibodies for human Ano5 makes it difficult to unravel the molecular function of Ano5 and the pathophysiology of Ano5-related muscular dystrophy. In this study, we demonstrate that the mAb N421A/85 specifically recognizes human Ano5 for western blot and immunofluorescence staining applications.

Using the recombinant Ano5 fusion construct, we observed several specific bands together with the full-length band. One larger band migrated at ~280 kDa, which is likely the dimeric form of the fusion protein. The other members of the anoctamin family such as Ano1, 2, and 6 have been shown to form dimers, and a dimerization domain located within the N-terminus has been defined in Ano1. The dimeric formation of Ano1, 2, and 6 appears to be sensitive to SDS; however, the potential dimer of Ano5 is resistant to SDS as it is still present in denaturing SDS-PAGE. This suggests that the transmembrane domains of Ano5 may also participate in dimer formation. Further experiments would be required to

determine the domains essential for the dimeric formation of Ano5 and the role of the dimeric architecture in its function.

We also observed several smaller bands of the Ano5 fusion construct using either anti-FLAG, anti-GFP, or N421/85 antibody. In particular, an N-terminal fragment of ∼49 kDa is consistently observed using anti-FLAG and N421/85 antibodies. In control human biopsies, we did not observe a specific band corresponding to the full-length Ano5 (predicted to be ∼107 kDa) with the N421/85 mAb. Instead, we observed a specific band ∼49 kDa, which was not present in three patients with confirmed mutations in *ANO5*. The lack of full-length Ano5 does not appear to be caused by non-specific degradation during sample preparation as a 427 kDa dystrophin band (which is known to be prone to degradation) was clearly seen. These results suggest that Ano5 is very labile and may undergo rapid proteolysis, which is consistent with a previous report showing that Ano5 is rapidly degraded via the proteasome pathway [14]. The biological significance of the 49 kDa N-terminal fragment and the other potential N-, C-, and internal fragments remains to be determined. Interestingly, dysferlin, a muscle membrane repair protein that is involved in the development of LGMD2B and MMD1 with phenotypic similarity to *ANO5*-deficient muscular dystrophy, was cleaved by calcium-dependent calpain [32,33]. Ano5 has also been implicated in muscle membrane repair. Thus, it is possible that a common calcium-dependent cleavage process for both dysferlin and Ano5 in response to membrane injury is a pre-requisite event for their roles in membrane repair.

Our western blotting and immunofluorescence staining experiments clearly detect the expression of mutant/truncated Ano5 peptide(s) in one patient who carries a c.363 + 4A > G mutation in intron 6. This is the first evidence that mutant/truncated Ano5 peptide(s) indeed exist, which may be involved in the pathogenesis of Ano5-related muscular dystrophy. Recently, we and others generated several independent lines of mice with *Ano5* disruption. Interestingly, the *Ano5* knockout mice with gene disruption at exon 1 or exon 2 did not show detectable muscular dystrophy phenotype. Both mice also have no detectable expression of *Ano5* transcripts in their muscles. However, the third line of *Ano5* knockout mice produced by gene trapping between exons 8 and 9 developed mild muscle pathology with ∼20% truncated *Ano5* transcript expression. All these findings are consistent with the notion that mutant/truncated Ano5 peptides rather than the complete loss of Ano5 expression are pathogenic in mouse models.

In summary, our study identified a highly specific mAb for human Ano5. With this novel antibody, we demonstrated that mutant/truncated Ano5 peptides are strongly expressed in the muscle biopsy of a human patient with mutation in a splicing donor site, which likely contributes to the pathogenesis of Ano5-related muscular dystrophy.

Acknowledgements

Author contributions statement

JX, LX, and RH conceived the studies. JX and LX carried out experiments, analysed data and contributed equally. YG and YSL carried out experiments. SAM provided human patient biopsies and carried out experiments. All authors were involved in writing the paper and had final approval of the submitted and published versions.

References

1. Katoh M, Katoh M. GDD1 is identical to TMEM16E, a member of the TMEM16 family. *Am J Hum Genet* 2004; **75:** 927–928. Author reply 928–929.

2. Penttilä S, Palmio J, Suominen T, *et al*. Eight new mutations and the expanding phenotype variability in muscular dystrophy caused by ANO5. *Neurology* 2012; **78:** 897–903.

3. Liewluck T, Winder TL, Dimberg EL, *et al*. ANO5-muscular dystrophy: clinical, pathological and molecular findings. *Eur J Neurol* 2013; **20:** 1383–1389.

4. Savarese M, Di Fruscio G, Tasca G, *et al*. Next generation sequencing on patients with LGMD and nonspecific myopathies: findings associated with ANO5 mutations. *Neuromuscul Disord* 2015; **25:** 533–541.

5. Xu J, El Refaey M, Xu L, *et al*. Genetic disruption of Ano5 in mice does not recapitulate human ANO5-deficient muscular dystrophy. *Skelet Muscle* 2015; **5:** 43.

6. Gyobu S, Miyata H, Ikawa M, *et al*. A role of TMEM16E carrying a scrambling domain in sperm motility. *Mol Cell Biol* 2016; **36:** 645–659.

7. Griffin DA, Johnson RW, Whitlock JM, *et al*. Defective membrane fusion and repair in Anoctamin5-deficient muscular dystrophy. *Hum Mol Genet* 2016; **25:** 1900–1911.

8. Duran C, Hartzell HC. Physiological roles and diseases of Tmem16/Anoctamin proteins: are they all chloride channels? *Acta Pharmacol Sin* 2011; **32:** 685–692.

9. Park SH, Chung HK, Kim DJ, *et al*. Overexpression, crystallization and preliminary X-ray crystallographic analysis of the C-terminal cytosolic domain of mouse anoctamin 1. *Acta Crystallogr Sect F Struct Biol Cryst Commun* 2011; **67:** 1250–1252.

10. Brunner JD, Lim NK, Schenck S, *et al*. X-ray structure of a calcium-activated TMEM16 lipid scramblase. *Nature* 2014; **516:** 207.

11. Pedemonte N, Galietta LJ. Structure and function of TMEM16 proteins (anoctamins). *Physiol Rev* 2014; **94:** 419–459.

12. Yamamura H. [TMEM16 as calcium-activated chloride channels]. *Nihon Yakurigaku Zasshi* 2013; **142:** 144.

13. Hartzell HC, Yu K, Xiao Q, *et al*. Anoctamin/TMEM16 family members are Ca^{2+}-activated Cl^- channels. *J Physiol* 2009; **587:** 2127–2139.

14. Tran TT, Tobiume K, Hirono C, *et al*. TMEM16E (GDD1) exhibits protein instability and distinct characteristics in chloride channel/pore forming ability. *J Cell Physiol* 2014; **229:** 181–190.

15. Fallah G, Römer T, Detro-Dassen S, *et al*. TMEM16A(a)/anoctamin-1 shares a homodimeric architecture with CLC chloride channels. *Mol Cell Proteomics* 2011; **10:** M110.004697.

16. Pifferi S, Cenedese V, Menini A. Anoctamin 2/TMEM16B: a calcium-activated chloride channel in olfactory transduction. *Exp Physiol* 2012; **97:** 193–199.

17. Malvezzi M, Chalat M, Janjusevic R, *et al*. Ca2+-dependent phospholipid scrambling by a reconstituted TMEM16 ion channel. *Nat Commun* 2013; **4:** 2367.

18. Galindo BE, Vacquier VD. Phylogeny of the TMEM16 protein family: some members are overexpressed in cancer. *Int J Mol Med* 2005; **16:** 919–924.

19. Katoh M, Katoh M. Identification and characterization of TMEM16E and TMEM16F genes in silico. *Int J Oncol* 2004; **24:** 1345–1349.

20. Rock JR, Harfe BD. Expression of TMEM16 paralogs during murine embryogenesis. *Dev Dyn* 2008; **237:** 2566–2574.

21. Tsutsumi S, Inoue H, Sakamoto Y, *et al*. Molecular cloning and characterization of the murine gnathodiaphyseal dysplasia gene GDD1. *Biochem Biophys Res Commun* 2005; **331:** 1099–1106.

22. Mizuta K, Tsutsumi S, Inoue H, *et al*. Molecular characterization of GDD1/TMEM16E, the gene product responsible for autosomal dominant gnathodiaphyseal dysplasia. *Biochem Biophys Res Commun* 2007; **357:** 126–132.

23. Duran C, Qu Z, Osunkoya AO, *et al*. ANOs 3–7 in the anoctamin/Tmem16 Cl^- channel family are intracellular proteins. *Am J Physiol Cell Physiol* 2012; **302:** C482–C493.

24. Zhao P, Torcaso A, Mariano A, *et al*. Anoctamin 6 regulates C2C12 myoblast proliferation. *PLoS One* 2014; **9:** e92749.

25. Bergeron JJM, Brenner MB, Thomas DY, *et al*. Calnexin: a membrane-bound chaperone of the endoplasmic reticulum. *Trends Biochem Sci* 1994; **19:** 124–128.

26. van der Kooi AJ, ten Dam L, Frankhuizen WS, *et al*. ANO5 mutations in the Dutch limb girdle muscular dystrophy population. *Neuromuscul Disord* 2013; **23:** 456–460.

27. Vihola A, Luque H, Savarese M, *et al*. Diagnostic anoctamin-5 protein defect in patients with ANO5-mutated muscular dystrophy. *Neuropathol Appl Neurobiol*. 2017; doi:10.1111/nan.12410.

28. Reese MG, Eeckman FH, Kulp D, Haussler D. Improved splice site detection in Genie. *J Comput Biol* 1997; **4:** 311–323.

29. Brunak S, Engelbrecht J, Knudsen S. Prediction of human mRNA donor and acceptor sites from the DNA sequence. *J Mol Biol* 1991; **220:** 49–65.

30. Vaz-Pereira S, Dansingani K, Holder GE, *et al*. Macular dystrophy presenting in one of two siblings with limb-girdle muscular dystrophy type 2L due to mutation of ANO5. *Eye* 2014; **28:** 102–104.

31. Sarkozy A, Hicks D, Hudson J, *et al*. ANO5 gene analysis in a large cohort of patients with anoctaminopathy: confirmation of male prevalence and high occurrence of the common exon 5 gene mutation. *Hum Mutat* 2013; **34:** 1111–1118.

32. Redpath GMI, Woolger N, Piper AK, *et al*. Calpain cleavage within dysferlin exon 40a releases a synaptotagmin-like module for membrane repair. *Mol Biol Cell* 2014; **25:** 3037–3048.

33. Lek A, Evesson FJ, Lemckert FA, *et al*. Calpains, cleaved mini-dysferlinC72, and L-type channels underpin calcium-dependent muscle membrane repair. *J Neurosci* 2013; **33:** 5085–5094.

SUPPLEMENTARY MATERIAL ONLINE

Figure S1. Epifluorescence imaging of human and mice ANO5 in 293AD cells

Figure S2. Screening of the anti-ANO5 antibodies by western blotting analysis

Figure S3. Screening of the anti-ANO5 antibodies in 293AD cell lines stably expressing mouse ANO5

Figure S4. Fluorescence imaging of recombinant constructs expressing truncated human Ano5 tagged with FLAG and GFP

Figure S5. Confocal imaging analysis of Ano5 and calnexin in the skeletal muscle cryosections of human patients

Figure S6. Sanger sequencing of the star-highlighted RT-PCR product shown in panel B of Figure 6

Table S1. Primer sequences

Table S2. Primary antibodies used for western blotting